

Antibiotics

How to cite: *Angew. Chem. Int. Ed.* **2022**, *61*, e202206168

International Edition: doi.org/10.1002/anie.202206168

German Edition: doi.org/10.1002/ange.202206168

A Specialized Polythioamide-Binding Protein Confers Antibiotic Self-Resistance in Anaerobic Bacteria

Finn Gude, Evelyn M. Molloy, Therese Horch, Maria Dell, Kyle L. Dunbar, Jana Krabbe, Michael Groll,* and Christian Hertweck*

Abstract: Understanding antibiotic resistance mechanisms is central to the development of anti-infective therapies and genomics-based drug discovery. Yet, many knowledge gaps remain regarding the resistance strategies employed against novel types of antibiotics from less-explored producers such as anaerobic bacteria, among them the Clostridia. Through the use of genome editing and functional assays, we found that CtaZ confers self-resistance against the copper chelator and gyrase inhibitor closthoamide (CTA) in *Ruminiclostridium cellulolyticum*. Bioinformatics, biochemical analyses, and X-ray crystallography revealed CtaZ as a founding member of a new group of GyrI-like proteins. CtaZ is unique in binding a polythioamide scaffold in a ligand-optimized hydrophobic pocket, thereby confining CTA. By genome mining using CtaZ as a handle, we discovered previously overlooked homologs encoded by diverse members of the phylum Firmicutes, including many pathogens. In addition to characterizing both a new role for a GyrI-like domain in self-resistance and unprecedented thioamide binding, this work aids in uncovering related drug-resistance mechanisms.

Introduction

Most natural environments harbor a remarkably complex collection of microorganisms,^[1] where bacteria must compete with their neighbors for space and resources.^[2] One way in which bacteria do this is by producing antibiotic natural products to inhibit susceptible competitors.^[3] Antibiotic-producing bacteria require a means of protection against suicide caused by the toxic effects of the antibiotic, which is most often mediated by self-resistance genes.^[4] The self-resistance strategies employed by antibiotic-producing bacteria include export and reduced influx of antibiotics, target modification, sequestration, and enzymatic inactivation,^[4b,5] which are mirrored in the counter-measures used by target organisms to defend themselves. This co-evolution of resistance can occur spontaneously, for example by alteration of the antibiotic target through mutation, or by horizontal transfer of resistance genes from other bacterial species.^[5] Unlike natural ecosystems where microbes produce low concentrations of multiple antibiotics, humans tend to deploy large concentrations of single antibiotics in medical and agricultural settings.^[6] Unfortunately, the accompanying promotion of antimicrobial resistance (AMR) inevitably goes on to limit the health and economic benefits of antibiotic use.

Still, antibiotics are our most important weapon to fight infectious diseases, with the vast majority in clinical use being either microbial natural products or their derivatives.^[7] While AMR has been an ongoing problem since the first clinical use of antibiotics, the rise in the number and diversity of resistant pathogens, including multidrug-resistant strains, is raising world-wide concern.^[8] In the majority of cases, the origins of the genetic determinants of clinical resistance can be traced to the self-protection mechanisms of antibiotic producers in natural environments.^[9]

The GyrI-like protein superfamily is of particular interest from the perspective of AMR since the conserved fold is functionally malleable, being capable of mediating various (self-)resistance strategies by differing modes of action.^[10] GyrI, the founding member of the superfamily, protects *Escherichia coli* against exogenously produced microcin B17 by inhibiting DNA gyrase, which is the cellular target of the bacteriocin.^[11] Furthermore, one subgroup contains enzymes that inactivate cyclopropyl antibiotics by hydrolysis, with two of these enzymes involved in the self-resistance of their producers.^[10c] Lastly, the transcriptional regulator BmrR from *Bacillus subtilis* binds diverse toxic compounds with its GyrI-like domain and subsequently

[*] F. Gude, Dr. E. M. Molloy, T. Horch, Dr. M. Dell, Dr. K. L. Dunbar, Dr. J. Krabbe, Prof. Dr. C. Hertweck
 Research Unit Biomolecular Chemistry, Leibniz Institute for Natural Product Research and Infection Biology, Hans Knöll Institute
 Adolf-Reichwein-Straße 23, 07745 Jena (Germany)
 E-mail: christian.hertweck@leibniz-hki.de

Prof. Dr. M. Groll
 Center for Protein Assemblies, Technical University of Munich
 Ernst-Otto-Fischer-Straße 8, 85747 Garching (Germany)
 E-mail: michael.groll@tum.de

Prof. Dr. C. Hertweck
 Faculty of Biological Sciences, Friedrich Schiller University Jena
 07743 Jena (Germany)

© 2022 The Authors. Angewandte Chemie International Edition published by Wiley-VCH GmbH. This is an open access article under the terms of the Creative Commons Attribution Non-Commercial NoDerivs License, which permits use and distribution in any medium, provided the original work is properly cited, the use is non-commercial and no modifications or adaptations are made.

resulting mutant strain could then be tested to verify whether CtaZ contributes to the CTA tolerance of *R. cellulolyticum*. *R. cellulolyticum* Δ *ctaZ* was generated by targeting *ctaZ* for incorporation of an in-frame nonsense mutation by CRISPR-nCas9 genome editing and verifying by restriction analysis (Figure 2A and Figure S3). We noted that the growth of *R. cellulolyticum* Δ *ctaZ* was impaired compared to the wild type only under conditions known to induce CTA production (Figure 2B),^[17a] presumably due to endogenous CTA production in the absence of CtaZ. We circumvented this issue by inactivating *ctaZ* in *R. cellulolyticum* Δ *ctaA*, a mutant devoid of production of CTA and all congeners,^[17a] thereby generating *R. cellulolyticum* Δ *ctaA* Δ *ctaZ* (Figure 2A and Figure S3). Notably, growth of the double mutant was not inhibited under CTA induction conditions (Figure 2B).

We proceeded to assess the effect of CtaZ deficiency on CTA susceptibility by *in vivo trans*-complementation experiments. We transformed *R. cellulolyticum* Δ *ctaA* Δ *ctaZ* with pMTL-*ctaZ*, an expression vector in which *ctaZ* is under the control of a constitutive promoter, and both *R. cellulolyticum* Δ *ctaA* and *R. cellulolyticum* Δ *ctaA* Δ *ctaZ* were transformed with the relevant empty vector (pMTL \emptyset) as controls. The susceptibility of the three stains to exogenous CTA was determined by the agar diffusion method (Figure 2C).^[23] Briefly, CTA solutions of differing concentrations were applied to paper discs on the surface of agar plates seeded with the test strains. CTA diffusion into the medium suppressed growth in the vicinity of the discs, resulting in measurable zones that increased in size with increasing CTA concentration. Minimum inhibitory concentration (MIC) values were calculated by analyzing the inhibition data using the dissipative model of antibiotic diffusion (Figure S4).^[24] We found that the double mutant (*R. cellulolyticum* Δ *ctaA* Δ *ctaZ* pMTL \emptyset) is 35-fold more sensitive to CTA than *R. cellulolyticum* Δ *ctaA* pMTL \emptyset (Figure 2C). This CTA-sensitive phenotype could be partially complemented by the provision of a plasmid-borne copy of *ctaZ*, as shown by the intermediate MIC of *R. cellulolyticum* Δ *ctaA* Δ *ctaZ* pMTL-*ctaZ* (Figure 2C). The incomplete restoration of CTA resistance by *trans* expression of *ctaZ* can conceivably be explained by i) insufficient *ctaZ* expression, for example due to inadequate plasmid copy number or a weaker promoter compared to that in the CTA BGC, and/or ii) the separation of *ctaZ* from native control disrupting the tightly regulated timing of expression typically observed for self-resistance genes.^[4] Nevertheless, the sensitivity of the *ctaZ*-deficient strain to CTA and its phenotypic complementation supports the proposal that *R. cellulolyticum* employs the GyrI-like protein CtaZ in self-resistance to CTA.

In light of our characterization of CtaZ as a self-resistance-conferring GyrI-like protein, we were curious as to how CtaZ endows *R. cellulolyticum* with CTA resistance. The other known self-resistance-conferring GyrI-like proteins, YtkR7 and C10R6, inactivate the products of their cognate BGCs by hydrolysis.^[10c] We reasoned that a sequence comparison with these enzymes could shed light on the manner of self-resistance imparted by CtaZ. There-

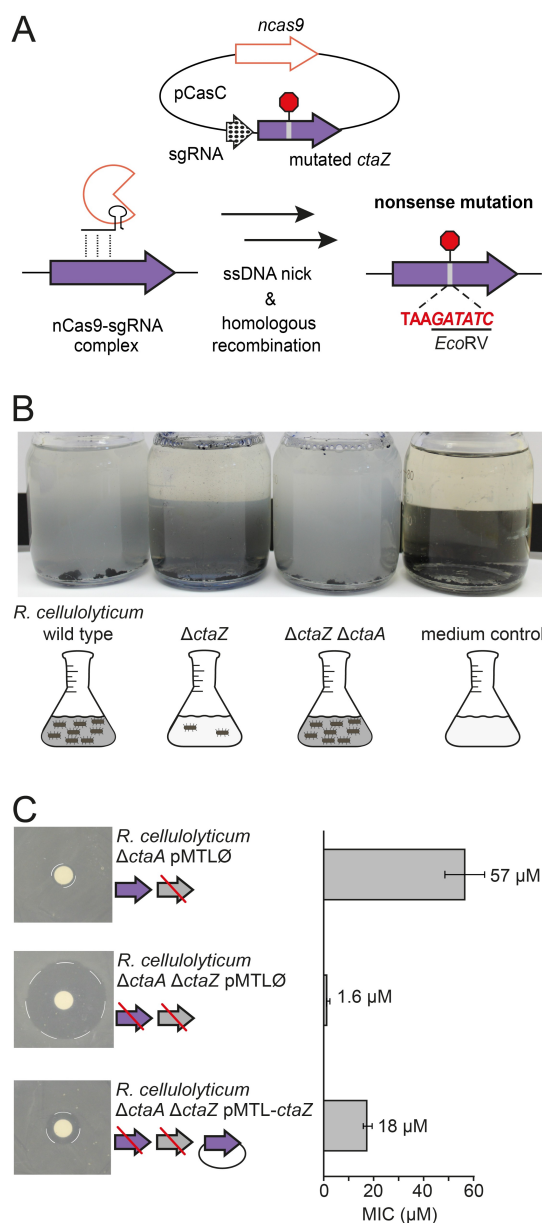


Figure 2. CtaZ contributes to the self-resistance of *R. cellulolyticum* to CTA. A) Scheme depicting the CRISPR-nCas9 strategy used to incorporate an in-frame nonsense mutation in *ctaZ* (Ccel_3263) of *R. cellulolyticum* and *R. cellulolyticum* Δ *ctaA* to generate the null mutants *R. cellulolyticum* Δ *ctaZ* and *R. cellulolyticum* Δ *ctaA* Δ *ctaZ*, respectively. The simultaneous introduction of an *EcoRV* recognition site enabled successful genome-editing to be detected by restriction digest of PCR products of the relevant region of *ctaZ*. B) Photos of cultures under CTA induction conditions demonstrate reduced growth of *R. cellulolyticum* Δ *ctaZ* compared to *R. cellulolyticum* wild type and *R. cellulolyticum* Δ *ctaA* Δ *ctaZ*. Black and white contrast in the background of the cultures is used to visualize differences in optical density. C) Left: Examples of the inhibition zones observed in lawns of the listed *R. cellulolyticum* strains in an agar diffusion assay using 40 μ M CTA. Dashed outlines show the zone borders. Red strikethroughs indicate inactivated genes. Right: Graphical representation of the minimum inhibitory concentrations (MICs) of CTA measured by agar diffusion method against the listed *R. cellulolyticum* strains. The MICs presented are averages determined from the analysis of three biological replicates (Figure S4), each consisting of two technical replicates, with error bars indicating \pm SD (see Table S6 for data summary).

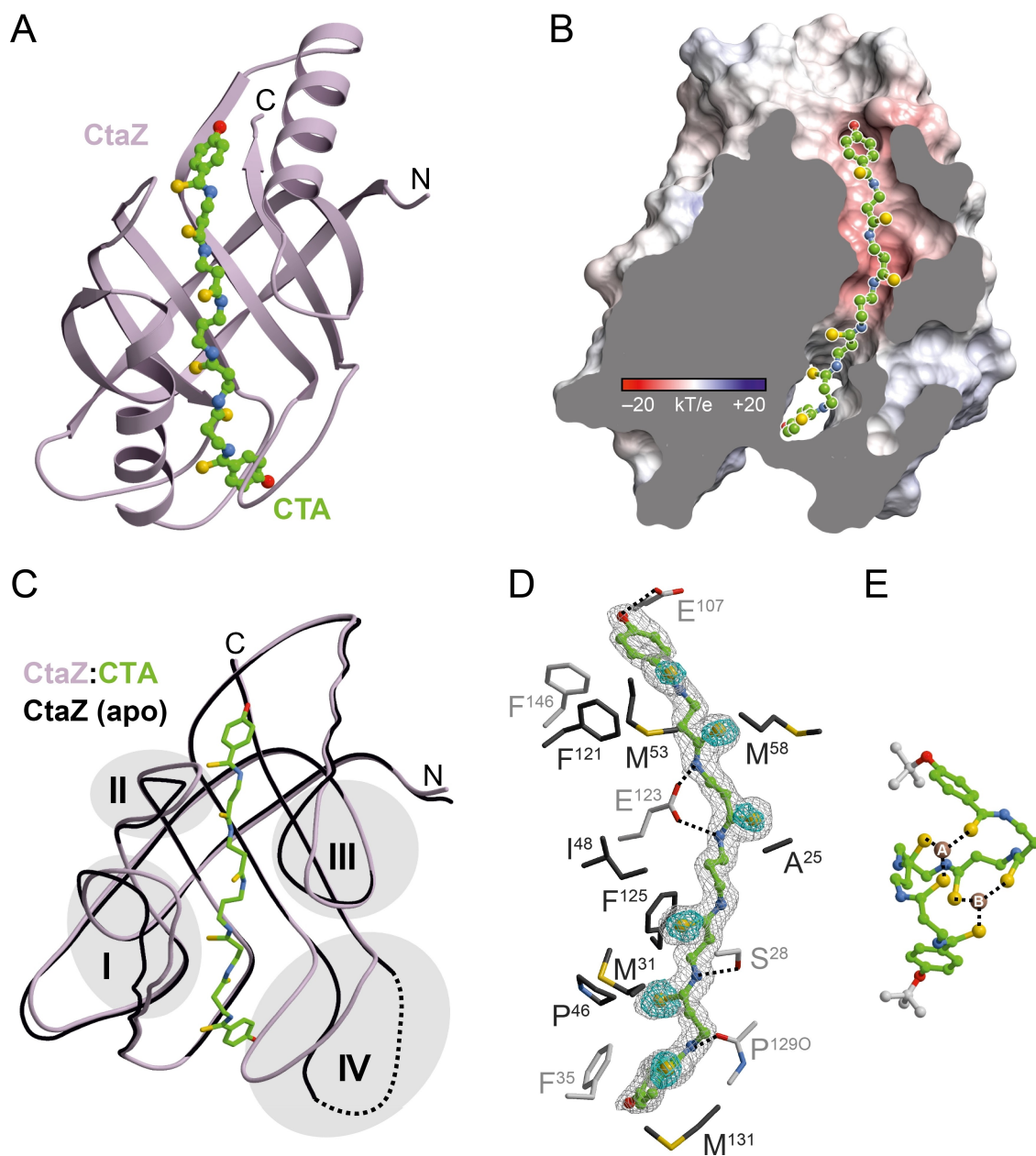


Figure 4. CTA is bound in a hydrophobic pocket of CtaZ. A) Ribbon diagram of CtaZ with its natural ligand CTA (carbon atoms in green; PDB ID: 7ZHJ). B) Surface cross section of the CtaZ:CTA-complex with colors indicating negative and positive electrostatic potentials. C) Structural superposition of the CtaZ:CTA complex (violet coils) and CtaZ(apo) (black, PDB ID: 7ZHE). Dots indicate a disordered loop region in CtaZ(apo). Conformational changes occur in four defined CtaZ-regions upon ligand binding: I (residues 19–32), II (residues 51–61), III (residues 94–100) and IV (residues 128–140). D) Close-up view of the CtaZ ligand binding site with depicted side chains engaged in binding. The $2F_o - F_c$ electron density map (grey mesh, contoured to 1.0σ) and the anomalous sulfur signal (cyan mesh, contoured to 5.0σ) are displayed for CTA. Residues involved in ligand stabilization by π -stacking and H-bonding (grey) and hydrophobic interactions (black) are highlighted. E) X-ray structure of $\text{Cu}_2(\text{tBu})_2\text{CTA}$ (Cu^I in brown spheres, CSD ID DIQPAW).^[16]

as well as the conformational changes induced by ligand binding. We found that CTA adopts an elongated conformation to occupy a pronounced groove (40 Å in length and 4 Å in width; Figure 4B) in the hydrophobic pocket of CtaZ, which we recognized in the CtaZ(apo) structure as likely capable of accommodating CTA. A comparative analysis of the structures of CtaZ(apo) and CtaZ:CTA provided a snapshot of the dynamics of CtaZ binding to CTA.

Substantial structural rearrangements occur in four defined regions of CtaZ after ligand binding (Figure 4C). Secondary structure elements of regions I (residues 19–32) and II (residues 51–61) are displaced by up to 4 Å to wrap around CTA. Side chains in the neighboring region III (residues 94–100) are shifted by 4 Å to facilitate the formation of a defined binding cavity. The most striking conformational changes induced by CTA-binding take place in the C-

terminal region IV (residues 128–140) of CtaZ. Compared to CtaZ(apo), side chains of region IV are displaced up to 6 Å in the CtaZ:CTA complex. Additionally, a loop that is disordered in CtaZ(apo) is rigidified in CtaZ:CTA as if to grasp one of the terminal *p*-hydroxybenzoic acid (PHBA) moieties of the ligand.

Although the linear conformation of the ligand in the binding pocket is energetically unfavorable, CTA is stabilized by extensive protein interactions due to its hydrophobic nature. Surprisingly, despite the symmetric architecture of CTA and its six thioamide repeats, all interactions with monomeric CtaZ are unique. The aliphatic β -alanine scaffold is buried in a narrow channel that minimizes ligand mobility. Furthermore, the terminal aromatic residues of CTA act as anchors: one PHBA undergoes strong π - π stacking with F35 whereas its counterpart is H-bonded to E107 and stabilized by Y103, F121 and F146 (Figure 4D). A special feature of the CtaZ:CTA structure is the unique coordination pattern of the polythiocarbonyl scaffold. There is a defined specificity pocket for each thioamide group, which is mainly formed by methionine and aromatic side chains. The nitrogen atoms of CTA form polar interactions with residues of CtaZ including S28 and E123, and the carbonyl oxygen of P129. Notably, the previously mentioned glutamate residue (E123), thought to be essential for small molecule binding (Figure 3A), contributes to the binding of CTA.

In compiling and interpreting this comprehensive structural information on the CtaZ-CTA interaction, we recognized two remarkable details in the CtaZ:CTA structure: i) The location of CTA in the binding pocket of CtaZ differs from previously reported structures of small molecules bound to GyrI-like domains. For the MDR transcriptional regulators BmrR^[27] and EcmrR^[26a] and the hydrolase Lin2189,^[10c] ligands are bound to one of three discrete binding sites distributed along the binding pocket (Figure S8), whereas CTA spans nearly the entire length of the binding groove with a contact area of 1034 Å² (Figure 4B). Therefore, the binding mode invoked by CtaZ to capture its ligand differs from that of other GyrI-like proteins. ii) CTA orientates lengthwise and rotated within the CtaZ binding groove, which is drastically different from the observed helical conformation of a CTA surrogate in complex with Cu^I (Figure 4E).^[16] From these contrasting conformations, we assume that CTA cannot complex Cu^I while bound to CtaZ. In conclusion, the collected crystal structures not only confirm that CtaZ is a binding protein of CTA, but also reveal a novel binding mode between a self-resistance-mediating GyrI-like protein and its natural ligand.

Inspired by our designation of CtaZ as a self-resistance-conferring binding protein, we aimed to gain insight into the distribution of similar proteins in the GyrI-like superfamily. To obtain an overview of the superfamily, we generated a sequence similarity network (SSN) based on members of the GyrI-like protein superfamily (PF06445; 39345 sequences) and homologs of CtaZ (Figure 5A and Figure S9).^[28] We used UniProt^[29] to construct the SSN because it is a resource for well-annotated and classified protein sequences and is integrated with the EFI-EST web tool. Collapsing proteins

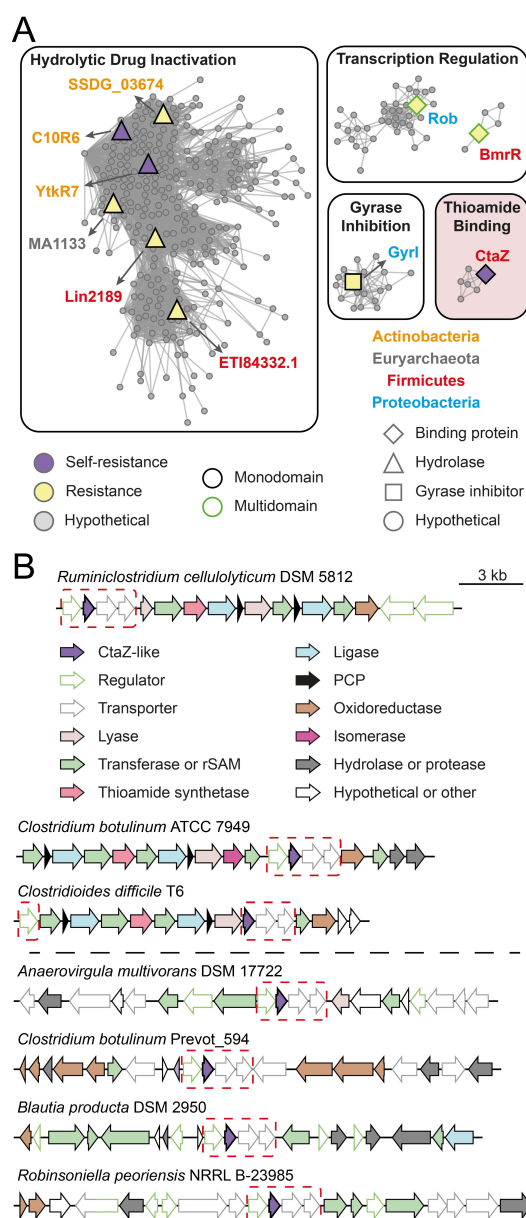


Figure 5. Homologs of CtaZ form a group in the GyrI-like protein superfamily and homologous genes are part of a putative resistance gene cassette. A) Sequence similarity network for CtaZ homologs and the GyrI-like protein superfamily (PF06445; proteins that share $\geq 50\%$ sequence identity over 80% of the sequence length are conflated; alignment score 40); only clusters containing members with characterized cellular functions are depicted (for full network see Figure S9). Nodes are colored based on a known resistance or self-resistance (encoded in biosynthetic gene clusters (BGCs)) function. Node outline color indicates the protein domain architecture, while the node shape corresponds to protein activity. Node labels correspond to a representative protein and are colored based on the phylum of the organism harboring the GyrI-like gene. B) Representative genetic loci that encode a CtaZ homolog (selected based on similarity to the CTA BGC or locus diversity). The CTA BGC (top) is shown for reference. Putative BGCs (middle) are separated by a dashed line from genetic loci not resembling BGCs (bottom). The putative resistance gene cassette is surrounded by a dashed box in each case.

with $\geq 50\%$ sequence identity over 80% of the sequence length into a single node resulted in a network composed of 4318 nodes. The superfamily clusters into 91 groups containing at least three nodes (covering 2773 nodes), with the remaining 1545 nodes being organized as pairs or singles. The hydrolase proteins cluster together in a large group, whereas the inhibitory (GyrI) and binding proteins (BmrR, Rob), including CtaZ, form separate individual groups. The groups reflect the diversity of cellular functions performed by members of the GyrI-like protein superfamily, which until now has comprised transcriptional regulation,^[12b,30] hydrolysis^[10c] and gyrase inhibition.^[21] CtaZ and its homologs form a group of previously undescribed proteins in the superfamily, alongside numerous uncharacterized groups (Figure S9). Overall, the SSN illustrates that the GyrI-like superfamily is far more complex than previously appreciated. Similar functional complexity is observed in other large and diverse protein families with a conserved structural motif but various cellular activities, such as the AAA + protein family.^[31] Therefore, with the identification of the CtaZ group we contribute to a better understanding of the cellular functions performed by members of the GyrI-like protein superfamily and lay the foundation for deciphering the cryptic functions of the remaining uncharacterized groups.

In addition to assessing the distribution of CtaZ homologs within the GyrI-like superfamily, we were interested in whether CtaZ homologs are used for self-resistance by other potential antibiotic producers. Therefore, we mined the genomic neighborhoods of *ctaZ* homologs for biosynthetic genes. To this end, BLASTp was used to identify 200 homologs of CtaZ in GenBank^[18] sharing minimum 44% sequence identity. We chose the GenBank database instead of UniProt because it contains a larger number of sequences and therefore provides a more accurate picture of the available data. Notably, we found that approximately one third of the CtaZ homologs are encoded in pathogenic members of the phylum Firmicutes. We next surveyed the genomic neighborhood surrounding the *ctaZ* homolog for genes encoding enzymes involved in secondary metabolite biosynthesis. The local genomic neighborhoods are highly diverse, with 2% of the *ctaZ* homologs found in loci similar to the CTA BGC (Figure 5B and Table S8). Surprisingly, most CtaZ homologs are encoded in loci that do not resemble typical BGCs. Therefore, it seems that CtaZ homologs are not commonly used in self-resistance. Interestingly, we noticed that in 96% of the cases the *ctaZ* homolog is co-localized with an upstream regulator and two downstream transporter genes, resembling a gene cassette (Figure 5B and Table S8). Export processes of cytotoxic molecules are commonly induced by transcriptional regulators and facilitated by transporters.^[32] Since genes encoding these types of proteins co-occur with *ctaZ* homologs in the vast majority of cases, we inferred that they may represent a functional unit responsible for protection against toxic molecules. Taken together, our findings on CtaZ expand the current picture of the cellular functions mediated by members of the GyrI-like superfamily to include antibiotic binding. In addition, our results on a putative resistance

gene cassette may indicate that these genes are involved in (self-)resistance to thioamide-possessing antibiotics, including in pathogenic bacteria.

Conclusion

In summary, we have characterized CtaZ as a self-resistance factor from *R. cellulolyticum* to the polythioamide antibiotic CTA. We demonstrated that CtaZ is a binding protein of CTA and establish it as the founding member of a new group in the GyrI-like protein superfamily. We observed a different conformation of CTA in complex with CtaZ compared to a CTA surrogate bound to Cu^I (Figure 4A and Figure 4E), intimating that CTA cannot complex Cu^I while bound to CtaZ. The complex structure suggests that CtaZ-bound CTA, in addition to being shielded from the intracellular copper pool, is prevented from interfering with the DNA gyrase of *R. cellulolyticum*. This work sets the basis for deciphering the molecular details of the CtaZ-mediated self-resistance mechanism and its regulation in the CTA producer *R. cellulolyticum*.

In light of our findings regarding the function of CtaZ, our current understanding of the role of GyrI-like proteins in AMR can be updated: i) The GyrI-like fold is crucial for binding of small molecules not only as part of multidomain transcriptional regulators (Rob and BmrR),^[12c,22b] which have an additional DNA-binding domain, but also in single domain proteins. ii) GyrI-like single domain proteins provide resistance not only by hydrolysis (YtkR7, C10R6)^[10c] or gyrase inhibition (GyrI),^[21] but also by small molecule binding (Figure 6). The GyrI-like fold is structurally distinct from that of other important multidrug-binding domains within the Alba and QacR classes.^[32b,33] Therefore, the detailed structural information on the CtaZ-CTA interaction contributes to a better understanding of the molecular factors that determine drug recognition by binding proteins.

The requirement for self-resistance in antibiotic producers provides a fertile ground for the evolution of AMR in non-producers due to the selective pressure exerted by microbial competition. Mobilization of these resistance genes to pathogenic bacteria is prompted by widespread antibiotic use.^[9a,c] Our bioinformatic survey uncovered numerous CtaZ homologs, thereby illuminating uncharted territory of the antibiotic resistome, which encompasses all antibiotic resistance genes in microorganisms.^[9c] It is essential that such antibiotic (self-)resistance genes of potential clinical significance are subject to biochemical characterization and bioinformatic surveying, in addition to monitoring emerging AMR.

This knowledge is critical to develop resistance management plans for both established antibiotics and new lead compounds. Given the undeniable connection between environmental and clinical resistance, we should perhaps be mindful that the newly identified CtaZ homologs and associated putative resistance gene cassette could potentially facilitate the transfer of AMR. In conclusion, our results not only address the mystery of self-resistance to CTA, but also

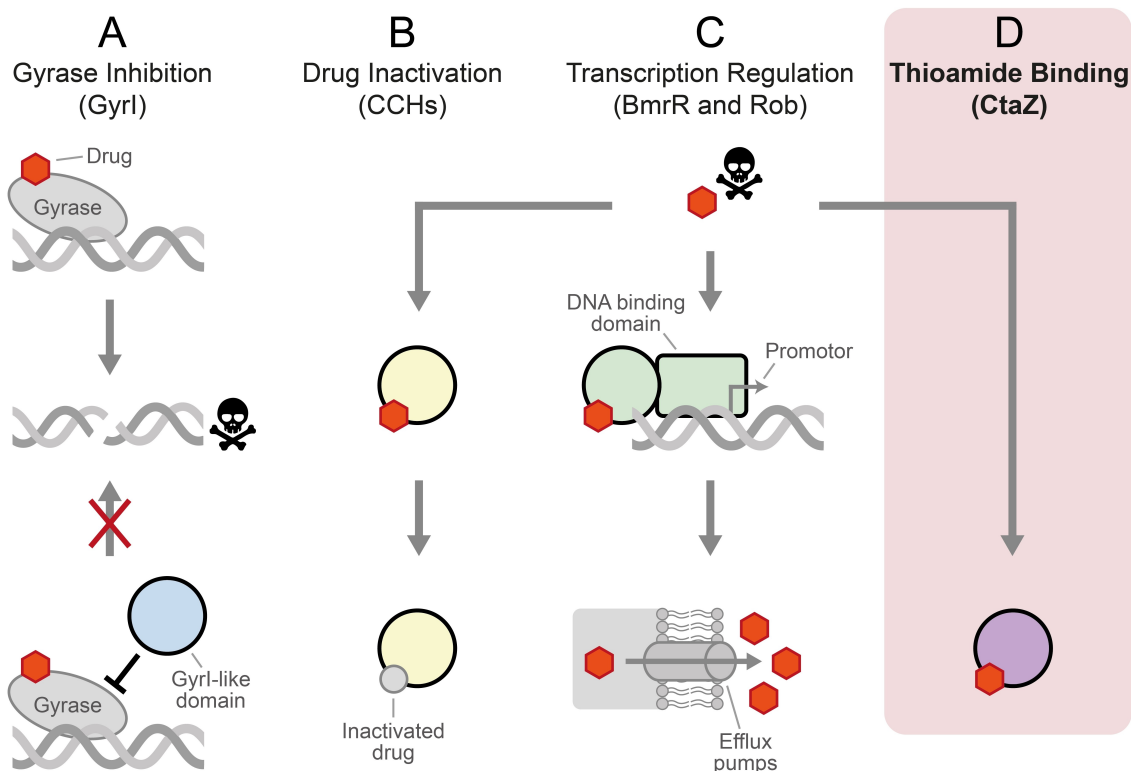


Figure 6. Overview of resistance strategies mediated by members of the Gyrl-like protein superfamily. Proteins are colored according to Figure 1C. A) Inhibition of DNA gyrase by Gyrl prevents the drug-induced formation of lethal DNA double-strand breaks. B) Members of the cyclopropanoid cyclopropyl hydrolase (CCH) group of Gyrl-like proteins, such as YtkR7 and C10R6, inactivate drugs by hydrolysis. C) Drug binding to the Gyrl-like domain of multidomain transcriptional regulators, such as BmrR and Rob, induces the transcription of genes encoding multidrug efflux pumps. D) The CTA binding protein CtaZ confers self-resistance to the antibiotic producer *R. cellulolyticum*.

serve as a starting point for the characterization of previously undetected resistance proteins.

Acknowledgements

CTA was provided by Florian Kloss. We thank Andrea Perner for MS measurements. We thank Ingrid Richter for helpful discussions on the phylogeny and Philipp Stephan and Hajo Kries for attempts to characterize the CtaZ-CTA interaction by ITC. We are grateful to the staff of the beamline X06SA at the Paul-Scherrer-Institute, Swiss Light Source, Villigen, Switzerland for assistance during data collection. We gratefully acknowledge financial support by the Deutsche Forschungsgemeinschaft (DFG, German Research Foundation), Cluster of Excellence “Balance of the Microverse” and Leibniz Award (to C.H.). In addition, financial support by the DFG, SFB 1309, project C01 (to M.G.) and the European Community’s Seventh Framework Program (FP7/2007–2013) under BioStruct-X (grant agreement no. 283570) is acknowledged. Open access funding enabled and organized by Projekt DEAL. Open Access funding enabled and organized by Projekt DEAL.

Conflict of Interest

The authors declare no conflict of interest.

Data Availability Statement

The data that support the findings of this study are available in the Supporting Information of this article.

Keywords: Antibiotics • Natural Products • Nonribosomal Peptide • Resistance • Thioamide

- [1] L. R. Thompson, J. G. Sanders, D. McDonald, A. Amir, J. Ladau, K. J. Locey, R. J. Prill, A. Tripathi, S. M. Gibbons, G. Ackermann, J. A. Navas-Molina, S. Janssen, E. Kopylova, Y. Vázquez-Baeza, A. González, J. T. Morton, S. Mirarab, Z. Zech Xu, L. Jiang, M. F. Haroon, J. Kanbar, Q. Zhu, S. Jin Song, T. Kosciolk, N. A. Bokulich, J. Lefler, C. J. Brislawn, G. Humphrey, S. M. Owens, J. Hampton-Marcell, D. Berg-Lyons, V. McKenzie, N. Fierer, J. A. Fuhrman, A. Clauset, R. L. Stevens, A. Shade, K. S. Pollard, K. D. Goodwin, J. K. Jansson, J. A. Gilbert, R. Knight, ‘The Earth Microbiome Project Consortium’, *Nature* **2017**, *551*, 457–463.

- [2] a) K. Faust, J. Raes, *Nat. Rev. Microbiol.* **2012**, *10*, 538–550; b) M. E. Hibbing, C. Fuqua, M. R. Parsek, S. B. Peterson, *Nat. Rev. Microbiol.* **2010**, *8*, 15–25.
- [3] M. M. Mullis, I. M. Rambo, B. J. Baker, B. Kiel Reese, *Front. Microbiol.* **2019**, *10*, 2518.
- [4] a) S. Mak, Y. Xu, J. R. Nodwell, *Mol. Microbiol.* **2014**, *93*, 391–402; b) K. H. Almabruk, L. K. Dinh, B. Philmus, *ACS Chem. Biol.* **2018**, *13*, 1426–1437.
- [5] J. M. A. Blair, M. A. Webber, A. J. Baylay, D. O. Ogbolu, L. J. V. Piddock, *Nat. Rev. Microbiol.* **2015**, *13*, 42–51.
- [6] a) S. R. Palumbi, *Science* **2001**, *293*, 1786–1790; b) E. Y. Klein, T. P. Van Boeckel, E. M. Martinez, S. Pant, S. Gandra, S. A. Levin, H. Goossens, R. Laxminarayan, *Proc. Natl. Acad. Sci. USA* **2018**, *115*, E3463–E3470.
- [7] D. J. Newman, G. M. Cragg, *J. Nat. Prod.* **2020**, *83*, 770–803.
- [8] a) S. B. Levy, B. Marshall, *Nat. Med.* **2004**, *10*, S122–S129; b) D. M. Livermore, *Clin. Microbiol. Infect.* **2004**, *10*, 1–9.
- [9] a) T. A. Wencewicz, *J. Mol. Biol.* **2019**, *431*, 3370–3399; b) V. M. D’Costa, C. E. King, L. Kalan, M. Morar, W. W. L. Sung, C. Schwarz, D. Froese, G. Zazula, F. Calmels, R. Debruyne, G. B. Golding, H. N. Poinar, G. D. Wright, *Nature* **2011**, *477*, 457–461; c) G. D. Wright, *Nat. Rev. Microbiol.* **2007**, *5*, 175–186.
- [10] a) V. Anantharaman, L. Aravind, *Proteins Struct. Funct. Bioinf.* **2004**, *56*, 795–807; b) A. Moreno, J. R. Froehlig, S. Bachas, D. Gunio, T. Alexander, A. Vanya, H. Wade, *Biochemistry* **2016**, *55*, 4850–4863; c) H. Yuan, J. Zhang, Y. Cai, S. Wu, K. Yang, H. C. S. Chan, W. Huang, W.-B. Jin, Y. Li, Y. Yin, Y. Igarashi, S. Yuan, J. Zhou, G.-L. Tang, *Nat. Commun.* **2017**, *8*, 1485.
- [11] a) M. R. Baquero, M. Bouzon, J. Varea, F. Moreno, *Mol. Microbiol.* **1995**, *18*, 301–311; b) A. Nakanishi, S. Imajoh-Ohmi, F. Hanaoka, *J. Biol. Chem.* **2002**, *277*, 8949–8954.
- [12] a) M. Ahmed, C. M. Borsch, S. S. Taylor, N. Vázquez-Laslop, A. A. Neyfakh, *J. Biol. Chem.* **1994**, *269*, 28506–28513; b) E. E. Heldwein, R. G. Brennan, *Nature* **2001**, *409*, 378–382; c) C. Fang, L. Li, Y. Zhao, X. Wu, S. J. Philips, L. You, M. Zhong, X. Shi, T. V. O’Halloran, Q. Li, Y. Zhang, *Nat. Commun.* **2020**, *11*, 6284.
- [13] T. S. Crofts, A. J. Gasparrini, G. Dantas, *Nat. Rev. Microbiol.* **2017**, *15*, 422–434.
- [14] a) T. Lincke, S. Behnken, K. Ishida, M. Roth, C. Hertweck, *Angew. Chem. Int. Ed.* **2010**, *49*, 2011–2013; *Angew. Chem.* **2010**, *122*, 2055–2057; b) F. Kloss, A. I. Chiriac, C. Hertweck, *Chem. Eur. J.* **2014**, *20*, 15451–15458; c) A. I. Chiriac, F. Kloss, J. Krämer, C. Vuong, C. Hertweck, H.-G. Sahl, *J. Antimicrob. Chemother.* **2015**, *70*, 2576–2588.
- [15] V. F. Miari, P. Solanki, Y. Hleba, R. A. Stabler, J. T. Heap, *Antimicrob. Agents Chemother.* **2017**, *61*, e00929–17.
- [16] F. Kloss, S. Pidot, H. Goerls, T. Friedrich, C. Hertweck, *Angew. Chem. Int. Ed.* **2013**, *52*, 10745–10748; *Angew. Chem.* **2013**, *125*, 10945–10948.
- [17] a) K. L. Dunbar, H. Büttner, E. M. Molloy, M. Dell, J. Kumpfmüller, C. Hertweck, *Angew. Chem. Int. Ed.* **2018**, *57*, 14080–14084; *Angew. Chem.* **2018**, *130*, 14276–14280; b) K. L. Dunbar, M. Dell, E. M. Molloy, F. Kloss, C. Hertweck, *Angew. Chem. Int. Ed.* **2019**, *58*, 13014–13018; *Angew. Chem.* **2019**, *131*, 13148–13152; c) K. L. Dunbar, M. Dell, F. Gude, C. Hertweck, *Proc. Natl. Acad. Sci. USA* **2020**, *117*, 8850–8858; d) K. L. Dunbar, M. Dell, E. M. Molloy, H. Büttner, J. Kumpfmüller, C. Hertweck, *Angew. Chem. Int. Ed.* **2021**, *60*, 4104–4109; *Angew. Chem.* **2021**, *133*, 4150–4155.
- [18] K. Clark, I. Karsch-Mizrachi, D. J. Lipman, J. Ostell, E. W. Sayers, *Nucleic Acids Res.* **2016**, *44*, D67–D72.
- [19] G. M. Boratyn, A. A. Schäffer, R. Agarwala, S. F. Altschul, D. J. Lipman, T. L. Madden, *Biol. Direct* **2012**, *7*, 12.
- [20] F. Gabler, S.-Z. Nam, S. Till, M. Mirdita, M. Steinegger, J. Söding, A. N. Lupas, V. Alva, *Curr. Protoc. Bioinf.* **2020**, *72*, e108.
- [21] M. Chatterji, V. Nagaraja, *EMBO Rep.* **2002**, *3*, 261–267.
- [22] a) E. E. Zheleznova, P. N. Markham, A. A. Neyfakh, R. G. Brennan, *Cell* **1999**, *96*, 353–362; b) H. J. Kwon, M. H. J. Bennik, B. Demple, T. Ellenberger, *Nat. Struct. Biol.* **2000**, *7*, 424–430.
- [23] E. P. Abraham, E. Chain, C. M. Fletcher, A. D. Gardner, N. G. Heatley, M. A. Jennings, H. W. Florey, *Lancet* **1941**, *238*, 177–189.
- [24] B. Bonev, J. Hooper, J. Parisot, *J. Antimicrob. Chemother.* **2008**, *61*, 1295–1301.
- [25] S. Bachas, C. Eginton, D. Gunio, H. Wade, *Proc. Natl. Acad. Sci. USA* **2011**, *108*, 11046–11051.
- [26] a) Y. Yang, C. Liu, W. Zhou, W. Shi, M. Chen, B. Zhang, D. G. Schatz, Y. Hu, B. Liu, *Nat. Commun.* **2021**, *12*, 2702; b) L. Holm, *Methods Mol. Biol.* **2020**, *2112*, 29–42.
- [27] K. J. Newberry, J. L. Huffman, M. C. Miller, N. Vazquez-Laslop, A. A. Neyfakh, R. G. Brennan, *J. Biol. Chem.* **2008**, *283*, 26795–26804.
- [28] a) J. A. Gerlt, J. T. Bouvier, D. B. Davidson, H. J. Imker, B. Sadkhin, D. R. Slater, K. L. Whalen, *Biochim. Biophys. Acta, Proteins Proteomics* **2015**, *1854*, 1019–1037; b) R. Zallot, N. O. Oberg, J. A. Gerlt, *Curr. Opin. Chem. Biol.* **2018**, *47*, 77–85.
- [29] UniProt Consortium, *Nucleic Acids Res.* **2019**, *47*, D506–D515.
- [30] E. Y. Rosenberg, D. Bertenthal, M. L. Nilles, K. P. Bertrand, H. Nikaido, *Mol. Microbiol.* **2003**, *48*, 1609–1619.
- [31] J. Snider, G. Thibault, W. A. Houry, *Genome Biol.* **2008**, *9*, 216.
- [32] a) J. F. Martín, J. Casqueiro, P. Liras, *Curr. Opin. Microbiol.* **2005**, *8*, 282–293; b) M. A. Schumacher, M. C. Miller, S. Grkovic, M. H. Brown, R. A. Skurray, R. G. Brennan, *Science* **2001**, *294*, 2158–2163.
- [33] a) L. Rostock, R. Driller, S. Grätz, D. Kerwat, L. von Eckardstein, D. Petras, M. Kunert, C. Alings, F.-J. Schmitt, T. Friedrich, M. C. Wahl, B. Loll, A. Mainz, R. D. Süßmuth, *Nat. Commun.* **2018**, *9*, 3095; b) A. Sikandar, K. Cirnski, G. Testolin, C. Volz, M. Brönstrup, O. V. Kalinina, R. Müller, J. Koehnke, *J. Am. Chem. Soc.* **2018**, *140*, 16641–16649.

Manuscript received: April 27, 2022

Accepted manuscript online: July 19, 2022

Version of record online: August 3, 2022